Tumor Targeting In Vivo and Metabolic Fate of 5-[Iodine-125]Iodo-2′-Deoxyuridine Following Intratumoral Injection in Patients with Colorectal Cancer

Giuliano Mariani, Andrea Cei, Paola Collecchi, Janina Baranowska-Kortylewicz,* Annick D. Van den Abbeele, Lorella Di Luca, Rossella Di Stefano, Paolo Viacava, Ezio M. Ferdeghini, Sonia Di Sacco, Piero A. Salvadori, Generoso Bevilacqua, S. James Adelstein, Franco Mosca and Amin I. Kassis

CNR Institute of Clinical Physiology at the University of Pisa, Nuclear Medicine Center, Institute of General and Vascular Surgery and Institute of Pathological Anatomy of the University of Pisa, Pisa, Italy; IST, National Cancer Institute, Genoa, Italy; Department of Radiology (Nuclear Medicine), Shields Warren Radiation Laboratory, Harvard Medical School, Boston, Massachusetts

Previous studies have demonstrated the tumor-targeting potential of radioiodinated 5-iodo-2′-deoxyuridine (IUdR) in experimental animal models following direct intratumoral or intracavitary administration. The aim of this study was to measure the tumor uptake and metabolic fate of 5-[^{125}I]iodo-2′-deoxyuridine ([^{125}I]IUdR) in humans after a single intratumoral injection. Ten patients with colorectal cancer were injected intratumorally with [^{125}I]IUdR (0.24–3.9 MBq) during endoscopy 24 hr before ablative surgery. Blood and urine samples were collected up to 72 hr after [^{125}I]IUdR injection. Following resection, the radioactivity in the tumor and the surrounding tissues was measured in a gamma counter, and microautoradiography was performed on semi-thin tissue sections to assess localization of the radiopharmaceutical at the cellular level. An average of 0.234% of the injected dose was present per gram of tumor (range 0.009–0.918, median value 0.147), and tumor-to-nontumor radioactivity incorporation ratios were high for colonic mucosa when the nontumor tissue was taken at 1 cm (mean 629, range 27–2391) and 15 cm (mean 2387, range 122–12674) from the injection site. Microautoradiography confirmed these high tumor-to-nontumor ratios and demonstrated localization of [^{125}I]IUdR in the tumor cell nuclei. These results suggest that radioiodinated IUdR might have potential as a tumor-targeting agent in humans, provided homogeneous intratumoral distribution of the radiopharmaceutical by a suitable route of loco-regional administration can be achieved.

J Nucl Med 1993; 34:1175–1183

Received Oct. 13, 1992; revision accepted Mar. 18, 1993.
For correspondence or reprints contact: Giuliano Mariani, MD, CNR Institute of Clinical Physiology at the University of Pisa, Via P. Savi 8, I-56126 Pisa, Italy.
*Current address: Dept. of Radiology, University of Nebraska Medical Center, Omaha, NE.

Recent studies have revived interest in the use of radiohalogenated synthetic thymidine analogues for in vivo tumor targeting (*1–5*). It has been shown that 5-iodo-2′-deoxyuridine (IUdR) is retained over a relatively long time in cell nuclei upon its active incorporation into the DNA of dividing mammalian cells (*6–10*) where it may also exert some radiosensitizing activity (*11,12*) whose clinical potential is currently being investigated (*13,14*). Rapid metabolic degradation of these compounds (*15–21*) and their nonselective uptake into all dividing cells in the body (whether they be normal or tumor cells) have so far constituted the main drawbacks to their use for in vivo tumor targeting following systemic administration. It is therefore not surprising that attempts at tumor imaging by external scanning after intravenous administration of radiohalogenated thymidine analogues (labeled with either ^{82}Br or ^{131}I) have generated rather disappointing results (*22,23*). On the other hand, experimental studies in animal tumor models have demonstrated that locoregional administration of radioiodinated IUdR (by direct intratumoral injection or by intracavitary administration) is followed by a highly efficient incorporation of the radiopharmaceutical in tumor cells (*1–5,24*).

The aim of the present work was to evaluate the in vivo uptake and metabolic fate of [^{125}I]IUdR in humans after intratumoral injection. For this purpose, radiolabeled IUdR was injected intratumorally during endoscopy in patients with colon cancer scheduled for ablative surgery. Aware that a single intratumoral injection is not a practical way to achieve homogeneous tracer distribution within the tumor, we specifically designed this study to: (a) demonstrate that radioiodinated IUdR is incorporated into the nuclei of tumor cells next to the injection site under these

TABLE 1
Patients' Clinical Data and Histopathologic Staging/Grading

Patient no.	Age (yr)	Sex	Site	Size (cm)	Dukes*	Histopathology staging	Grading	M/10 HPF†
ML01	75	F	Sigmoid	2 × 2	B1	pT2N0	G2	17
CF02	87	F	Left colon	3 × 4	B2	pT3N0	G2	12
AR03	51	F	Left colon	4.5 × 6	B2	pT3N0	G2	20
CM04	53	F	Rectum	2.5 × 5	C2	pT3N2	G3	20
TC06	67	M	Rectum	4.5 × 5.5	B2	pT3N0	G2	13
CS07	66	M	Rectum	3 × 3	B2	pT3N0	G2	5
TM08	78	M	Rectum	3 × 5	B2	pT3N0	G2	5
BL11	70	F	Sigmoid	2 × 3	C1	pT2N1	G2	35
GG13	78	M	Sigmoid	4 × 4	C2	pT3N2	G4	22
AP19	62	F	Sigmoid	1.5 × 2.5	B2	pT2N0	G2	8

*Modified by Astler and Coller (The prognostic significance of direct extension of carcinoma of the colon and rectum. *Ann Surg* 1954;139:846–851).
†Number of mitoses per 10 high-power fields.

experimental conditions, (b) provide a quantitative evaluation of tumor versus nontumor incorporation in an environment in which both normal and cancer cells have a high proliferative index and (c) determine the metabolic fate of this radiopharmaceutical in humans following intratumoral injection.

MATERIALS AND METHODS

Radiotracer

No-carrier-added sterile [^{125}I]IUdR (specific activity 74 TBq/mmol [2000 Ci/mmol]) was purchased from Amersham Plc (Amersham, United Kingdom). The compound was routinely injected within 1 wk after labeling (radiochemical purity over 95%; not more than 5% radioiodide on chromatography). After testing for the absence of pyrogens, the tracer was dissolved in physiologic saline (0.15 *M* NaCl) for direct tumor injection during endoscopy.

Patients and Protocol

Ten patients (six women and four men, 51–87 yr of age) scheduled for ablative surgery for colorectal adenocarcinoma were enrolled in the study. Table 1 details the location, extent, histologic gradings and staging of neoplastic disease for these patients.

The protocol was approved by the Joint Ethical Committee for the Protection of Human Subjects in Medical Research of the University of Pisa Medical School and the University-affiliated Hospital of Pisa and was subject to a limitation on normal tissue sampling (see below). Before giving their consent, patients were informed that the principal aim of the investigation was to assess the tumor-targeting capabilities of the proposed procedure and that treatment of their disease would not be affected by the results of the procedure itself.

Beginning 48 hr before [^{125}I]IUdR administration, patients were given potassium iodide (10 drops of a saturated KI solution three times a day) for a total of 10 days to prevent thyroidal accumulation of ^{125}I released during metabolic degradation of the injected tracer. On the day before scheduled surgery, intratumoral injection of [^{125}I]IUdR was performed during endoscopy (flexible fiber-optic colonoscope model CF1T10I, Olympus, Fukuo, Tokyo, Japan) using a catheter designed for esophageal vein sclerosing injections (4-mm, 23-gauge needle). A total volume of 0.5–1 ml (measured by the double-weighing technique using an electronic scale with 0.01 mg accuracy) containing about 4–15 MBq of [^{125}I]IUdR (100–400 μCi) was injected at the intraluminal growing edge of the tumor (in its most distal portion) in two to four separate injections a few millimeters apart. Endoscopic observation during injection revealed that a substantial fraction of the injectate leaked out at the injection site. Meticulous saline washings of the surface of the infused area and of the syringe and catheter used for injection resulted in the recovery of 58%–95% (mean 82%) of the radioactivity withdrawn from the storage vial. The actual injected dose (calculated as the difference between the dose withdrawn from the stock solution and the cumulative recovered radioactivities) was therefore equal to about 0.24 to 3.9 MBq (6.4–106 μCi).

Vital signs (pulse rate, arterial blood pressure, respiration, body temperature) were monitored during the first 24 hr after intratumoral injection of [^{125}I]IUdR, at which time patients underwent surgery and were then monitored according to routine intensive care procedures. No adverse reaction of any kind was observed in any of the patients participating in the study.

Heparinized venous blood samples were routinely taken at 15 and 30 min and at 1, 2, 3, 6, 12, 24, 36, 48 and 72 hr after intratumoral injection to derive clearance curves. Urine samples (pooled at 24-hr intervals) were collected over the same period to evaluate removal of radioactivity from the body.

Samples taken from the surgical specimen were used for radioactivity measurements and microautoradiography. In addition, in the first two patients, surgical biopsies were taken from the liver (edge biopsy) and from the bone marrow (iliac crest) during the main surgical procedure. The Ethical Committee did not grant further authorization for tissue sampling from these sites since no significant radioactivity was detectable in these specimens. Finally, the gallbladder and bile were obtained for radioactivity measurements in two patients for whom cholecystectomy had been scheduled at the same time as tumor ablative surgery because of known cholelithiasis.

Processing of Tissue Samples for Assessment of Radioactivity

After repeated washing with physiologic saline, the entire tumor was systematically dissected into 0.2- to 0.8-g specimens, working from the endoluminal to the serosal surface (thus also frequently including some normal tissue components that were macroscopically evident). These "tumor" samples (as well as

normal tissue samples taken as detailed below) were blotted dry on filter paper (except for the bone marrow), weighed and placed in 10% formalin using propylene test tubes suitable for counting in an automatic gamma counter (1282 Compugamma CS, LKB-Wallac, Wallac Oy, Turku, Finland). This equipment had a measured counting efficiency of 85% for ^{125}I. Tissue samples were counted for 20–60 min with counting errors below 1% (typically 0.1%–0.3%). Radioactivity counting of all tumor samples served to identify the areas adjacent to the injection sites that were not otherwise identifiable except for the generic location at the distal end of the tumor, i.e., the portion best approached during endoscopy.

For each patient, the radioactive content of colonic mucosa taken both within 1 cm and at 15 cm from the injection site was also measured. In this regard, colonic mucosa within 1–4 cm from colorectal cancer is commonly defined as "transitional mucosa" (*25*) and is characterized by cell proliferation kinetics faster than mucosa more distant from the tumor, even if generally exhibiting normal appearance at conventional light microscopy (*26,27*). In addition, samples of the following normal tissues were similarly processed and counted for radioactive content: liver and iliac crest aspirates (n = 2), mesenteric fat from the injection area (n = 8), hyperplastic lymph nodes from the surgical area (n = 4) and gallbladder and bile (n = 2). The fraction of injected dose present in each sample and the tumor-to-nontumor radioactivity incorporation ratios were calculated and tissue samples with the highest radioactivity were selected for microautoradiography.

Microautoradiography

After alcohol dehydration, tissue samples were embedded in paraffin and sequentially sectioned (semi-thin sections, 3–4 μm thick), coated with NTB-2 emulsion (Kodak, diluted with distilled water 1:1.5), dried and stored at 4°C in light-tight boxes. Following exposure of at least 4 wk in the dark, the emulsions were developed (Kodak developer D-19b) for about 5 min at 19°C and fixed (Kodak Unifix or Kodak F-5 fixer) for 10 min. Finally, the slides were rinsed, stained with hematoxylin-eosin and mounted in Permount. Gamma counting of aliquots from the solutions used for tissue dehydration and for staining revealed minimal radioactivity contents, thus confirming earlier findings demonstrating that 95% of [^{125}I]IUdR is found to be incorporated into the nuclear DNA of labeled cells (*28*).

Microautoradiography was also performed on peripheral blood smears obtained from patients CF02 and AR03 at 1 and 2 hr, respectively, after intratumoral injection of [^{125}I]IUdR. Blood smears were fixed in 100% methanol, processed as described above and stained with Wright stain.

Microautoradiographs were analyzed with the aid of an image processing computer system (see Fig. 1). The microautoradiographic slides were placed on a uniformly illuminated surface, and a camera fitted with a Vidicon tube, a Canon lens Macro 50 mm (1:3.5) and a Canon extension tube FD25 was used to transfer a video image of the slides to an array processor-based computer for image processing (Mipron, Kontron, Munich, Germany). The analog-to-digital converter, running at 20 MHz, digitized the images into matrices of 1024 × 1024 pixels, 256 color levels each (using adequate "look-up" tables for pseudo-color rendering, see Fig. 1B). By means of the digitizing tablet and with the aid of a marker controlled by a track-ball, a contour was manually drawn to establish the boundaries of both the histologic preparation in toto and the tumor subset corresponding to the volume occupied by the injectate (identified by the blackened region in the microautoradiograph). The computer calculated the areas of the whole tissue slice and of the tumor subset in terms of number of pixels, and the subset-to-whole slice area ratio was then obtained.

Processing of Blood and Urine Samples

In order to derive blood clearance and urinary excretion rates, the radioactive contents of aliquots of blood/plasma and urine samples were measured. Blood samples were routinely allowed to equilibrate (2–3 hr at 4°C) to reach homogeneous radioactivity distribution before separating plasma. Immediately after separation, plasma sample aliquots as well as urine aliquots from three patients (ML01, AR03 and TM08) were lyophilized for later HPLC analysis, to evaluate the radioactive species present at various times after injection. In fact, stability experiments had shown that radioiodinated IUdR incubated with blood is slowly deiodinated, the tracer being degraded with a half-life of about 72 hr at 4°C. After reconstitution, the plasma samples were immediately processed for HPLC at 4°C in order to prevent any important phosphorolytic cleavage of radiolabeled IUdR by enzymatic activities (*29,30*).

Reconstituted urine samples (pooled from 0 to 24 hr and 24 to 48 hr, n = 6) were filtered through 0.22-μm Millipore filters and analyzed on a C18 reversed-phase HPLC column using CH_3OH/H_2O (20/80; flow rate: 1.0 ml/min) as the mobil phase. Samples with high radioactivity content were injected directly on the column after filtration. For samples with less radioactivity, the filtered urine samples were extracted with chloroform/tetrahydrofuran (5/1) (4 × 1 ml/ml urine) to remove any IUdR and metabolites soluble in organic solvents. The organic layer was then evaporated under a stream of nitrogen to a volume of about 100 μl and analyzed on a C18 column. The aqueous layer was treated with chloramine-T (0.1 mg/ml urine) to facilitate the extraction of oxidized ^{125}I with chloroform (4 × 0.5 ml). Aliquots of each fraction were counted. The iodide recovered in this second layer was reduced with 10 μl of an aqueous sodium metabisulfite solution (10 mg/ml) to prevent its loss during evaporation of the solvent to about 100 μl.

Reconstituted plasma samples collected at 1, 2 and 3 hr (n = 6) were treated in the following manner. To each sample, an equal volume of ethanol was added to precipitate proteins (10 min on ice). Samples were centrifuged at 3000 g for 20 min, the supernatant was Millipore filtered and aliquots (approximately 100 μl) were injected on the C18 column.

RESULTS

Tissue Radioactive Contents and Tumor-to-Nontumor Ratios

An average of 0.234% of the injected dose per gram (ID/g) of tissue (range 0.009–0.918, median value 0.147% ID/g) was measured at the injection site. Table 2 gives the values obtained for each patient as well as the tumor-to-nontumor radioactivity incorporation ratios for normal colonic mucosa within 1 cm and at 15 cm from the injection site. These tumor-to-colon ratios were high: within 1 cm, mean 629, median 547; at 15 cm, mean 2387, median 1276.

In the liver biopsy specimens obtained from Patients ML01 and CF02, barely detectable amounts of radioactivity (less than twice background) were found to be associated with liver parenchyma 24 hr after intratumor injection of [^{125}I]IUdR, which resulted in very high tumor-to-liver

TABLE 2
Tissue Counting and Microautoradiography Data

Patient no.	Tumor (%ID/g)	Tumor/Normal colon		Tumor-to-blood	Incorporation (% tumor cells)
		1 cm	15 cm		
ML01	0.308	758	2759	440	38.0
CF02	0.343	562	1885	330	41.7
AR03	0.097	532	1098	222	32.2*
CM04	0.009	27	122	16	†
TC06	0.918	2391	12674	168	53.0
CS07‡	0.046	849	1454	249	30.1
TM08	0.047	66	463	61	14.5
BL11	0.196	35	716	342	34.2
GG13	0.291	697	2066	536	34.0
AP19	0.082	375	637	113	20.0*
Mean ± s.e.m.	0.2337 ± 0.0898	629 ± 230	2387 ± 1235	248 ± 55.5	33.1 ± 4.0
Median	0.1465	547	1276	289.5	34.0

*Occasional radioactive incorporation by transitional epithelium.
†Autoradiography not performed because of low incorporation (7000 cpm/g tumor).
‡Surgery performed 72 hr after [^{125}I]IUdR injection.

ratios (13946 and 3142, respectively). The gallbladder wall of Patients ML01 and BL11 also had extremely low radioactive content (tumor-to-gallbladder ratios of 5838 and 494, respectively), whereas radioactivity in the bile of these two patients (tumor-to-bile ratios 403 and 103, respectively) was consistently higher than in the blood at the time of surgery (bile-to-blood ratios 1.13 and 3.31, respectively), thus suggesting an active biliary excretion mechanism. Unfortunately, these biliary radioactivities were too low for chromatographic identification of the radiochemical species.

The bone marrow biopsy was unsuccessful in Patient CF02, since only fatty material without any associated radioactivity was recovered. For Patient ML01, the radioactive content of the bone marrow was very low with a tumor-to-bone-marrow ratio of 1756 and a blood-to-bone-marrow ratio of 3.9 (despite the fact that the bone marrow material was not washed free of blood before weighing and counting the radioactivity). Finally, radioactivity incorporation was very low in the mesenteric fat samples taken in the vicinity of the injection site (average tumor-to-fat ratio 3532, range 1410–7383), whereas the average tumor-to-lymph node ratio for hyperplastic lymph nodes draining from the tumor was 567 (range 189–2127).

It should be noted, however, that the tumor uptake values listed in Table 2 underestimate actual radioactivity incorporation by the tumor per se. It was obvious in the microautoradiographs that the so-called "tumor" samples included normal intestinal wall components and that the distribution of radioactivity within the tumor was confined to a restricted volume around the injection sites. Computer-aided image analysis of microautoradiographs obtained with sequential sections showed that about 25% of the total tissue specimen (range ~10%–45%) corresponded on average to "tumor" actually exposed to the injectate (Fig. 1A–B). This volume had a roughly ellipsoidal shape within the tumor mass, but showed sometimes more irregular shapes due to either stromal connective structures limiting tracer diffusion around the injection site and/or the random cut of the surgical specimen.

Microautoradiography

Microautoradiography confirmed the very high tumor-to-nontumor ratios obtained by in vitro tissue counting and showed that within each tumor there were areas of high radioactivity (probably corresponding to the injection site), areas with lower uptake levels and areas virtually devoid of any radioactivity (distant from the injection site). Furthermore, radioactivity incorporated by the tumor cells was specifically associated with the nuclei of these cells (Fig. 2). Within tumor areas showing the highest uptake, the fraction of neoplastic cells with nuclear-associated radioactivity varied between 15% and 53% (mostly in the 30%–40% range, Fig. 3A, Table 2).

Normal appearing cryptal glands overlying the tumor (transitional mucosa, Fig. 3B) in some cases exhibited a very low incorporation of radioactivity, either at their luminal surfaces and/or towards the *lamina propria*. A somewhat higher incorporation by transitional mucosa was seen only in Patients AR03 and AP19, while radioactivity was occasionally observed within the tumoral stroma. Autoradiographs of the peripheral blood smears obtained in Patients CF02 and AR03 at the peak of circulating radioactivity showed some silver grains upon long-term exposure (4–6 mo). However, these grains were not associated with specific blood elements and all activity seemed to be background.

Radioactivity Kinetics in Plasma and Urine

Radioactivity in plasma rose quickly after intratumoral injection of [^{125}I]IUdR, reaching a peak at the 1-hr time point to correspond to about 4%–6% of the ID/liter of plasma. The decline in radioactivity followed monoexpo-

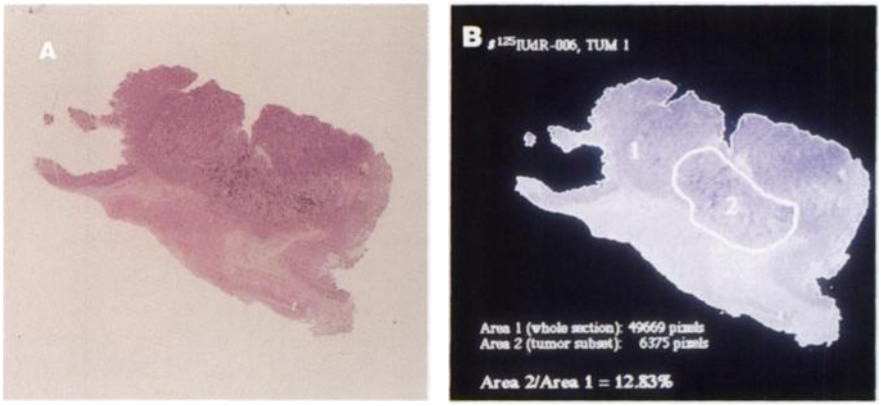

FIGURE 1. Example of computer-aided image analysis for microautoradiographs (magnifications ~2.8×). (A) Original tissue section after complete processing (development of photographic emulsion and staining with hematoxylin-eosin). The portion of tumor with radioactivity incorporation is clearly outlined as the darkened area, whereas the section includes both tumor and nontumor components (intestinal wall in lower left). (B) Image processing: Area "1" corresponds to entire surface of tissue section (49,669 pixels in this example) and was outlined by color-level segmentation. Area "2" (site of [^{125}I]IUdR injection, occupying only central lower part of tumor component) was delineated with the aid of a track-ball using low-magnification microscopy (10–25×) of the original section (A) as a guide as the area containing cells with overlapping high-density grains. The ratio of Area "2" to Area "1" is 0.1283 (or 12.83%).

nential, first-order kinetics at least up to 24 hr after injection (Fig. 4), with a mean half-life of 8.09 ± 1.92 hr (slope: 0.08971 ± 0.02057 hr^{-1}). As demonstrated by HPLC, virtually all of the radioactivity was in the form of free [^{125}I]iodide (≥98%), with the exception of the plasma samples at the 3-hr time point, where about 5% of the total radioactivity recovered was identified as undegraded [^{125}I]IUdR.

Urinary excretion of radioactivity accounted for 67.07 ± 6.47 %ID over the 3-day period following intratumoral administration of [^{125}I]IUdR. Most of the excretion took place within the first 48 hr postinjection (50.89 ± 8.02 %ID on Day 1, 15.10 ± 7.54 %ID on Day 2, 1.07 ± 0.10 %ID on Day 3). In two patients in whom urine collection was continued beyond 72 hr, additional recovery of excreted radioactivity was minimal (0.115 %ID and 0.075 %ID, respectively on Days 4 and 5 for Patient ML01; 0.08 %ID on Day 4 for Patient AR03). Of the radioactive species in the urine samples analyzed by HPLC, undegraded [^{125}I]IUdR accounted for a substantial fraction of radioactivity (18%–24% of total) in the first 24 hr. The remaining radioactivity excreted on Day 1 was [^{125}I]iodide, virtually the only radioactive species present in the Day 2 samples.

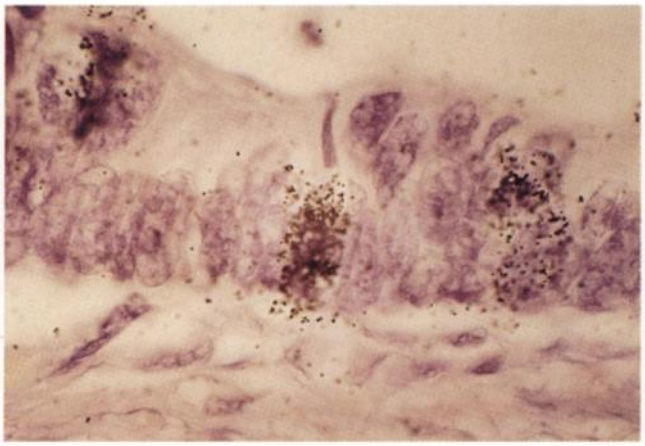

FIGURE 2. High magnification (~1020×) of a microautoradiographic section obtained after short-term exposure demonstrates radioactivity incorporation specifically in tumor cell nuclei.

DISCUSSION

Iodine-125, which decays predominantly (93%) by internal conversion following electron capture, demonstrates an Auger effect in which extremely low energy (<1 keV) electrons (mean of 20 per decay) are produced (*31*). This event deposits 10^9 rad/decay within a 20-nm sphere around the decaying atom (*10,32,33*). Experiments have shown that the decay of this isotope in the DNA of dividing mammalian cells leads to: (a) the efficient production of DNA double-strand breaks (DSB) (one decay = one DSB) (*34*); (b) an exponential reduction in cell survival with no shoulder (absence of repair) on the survival curve and high relative biological effectiveness (RBE) values (7.3) (*10,33–37*); and (c) an oxygen enhancement ratio (OER) of 1.4 (*37*) which is significantly smaller than the OER of 3 for x-ray exposure. In contrast, the decay of ^{125}I within cell cytoplasm (*33*), affixed to cell plasma membranes (*35*) or extracellularly (*10,32*) produces no extraordinary lethal effects and these survival curves: (a) resemble those observed with x-ray (have a distinct shoulder); (b) exhibit shallower slopes; and (c) have a low RBE (<2).

IUdR is a thymidine (TdR) analogue in which the 5-methyl group of TdR is replaced by iodine. Since the 5-methyl group and the iodine atom have similar van der Waals' radii, this substitution gives a compound that behaves remarkably like TdR (*6,10,38*). Within the cell, it is phosphorylated in a stepwise reaction (*39*) and incorporated into DNA, the latter process being proportional to exposure time and extracellular concentration (*10*). Once incorporated, most of the IUdR is retained for the life of the cell or its progeny (*6*), with some slow-rate deiodination occurring in vivo (*40*).

The use of IUdR in vivo creates several problems. The first relates to the matter of achieving high tumor-to-normal

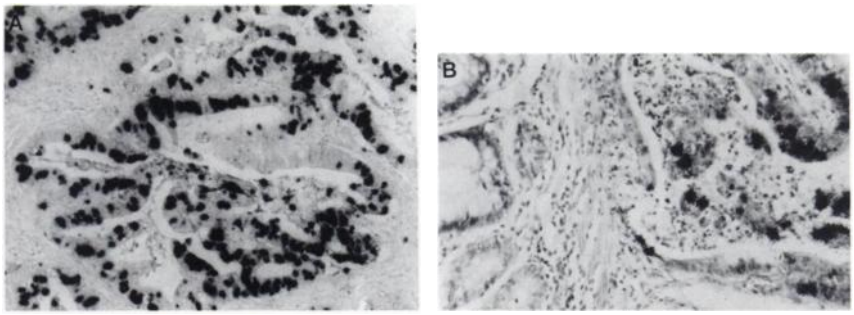

FIGURE 3. (A) Microautoradiograph shows active radioactivity incorporation by a fraction of tumor cells as high as ~40%–50% (magnification ~190×). (B) Higher magnification (~290×) shows no radioactivity incorporation in cryptal gland cells of normal appearing transitional mucosa (left) overlying a nest of tumor cells with intense radioactivity incorporation.

tissue ratios in the face of high in vivo instability [the half-life of IUdR in the circulation in humans is <5 min (*21*) and in mice 7 min (*20*)]. The second relates to the uptake of IUdR by actively proliferating normal cell renewal systems (bone marrow, gut) and the consequent possibility of normal tissue toxicity. Both of these problems may be solved by direct (e.g., locoregional) drug administration. A third problem shared with other cycle-dependent drugs is that IUdR can only label cells in the DNA synthetic S phase. However, earlier studies (*1,3,5,24*) have clearly demonstrated that the locoregional administration of radiolabeled IUdR in several animal tumor models leads to the scintigraphic detection and therapy of tumors.

The present results obtained in humans confirm the highly favorable tumor-targeting properties of radioiodinated IUdR previously shown in animal tumor models following its locoregional administration (*1,3,5,24*). In particular, samples taken from tumors surgically resected 24 hr after intratumoral injection of [^{125}I]IUdR demonstrate that the fraction of administered radioactivity that remains associated with the tumor at the injection site is quite high. The average minimal estimate of 0.234 %ID/g of tumor (range 0.009–0.918 %ID/g not corrected for that portion of the tumor actually exposed to the injected [^{125}I]IUdR) is

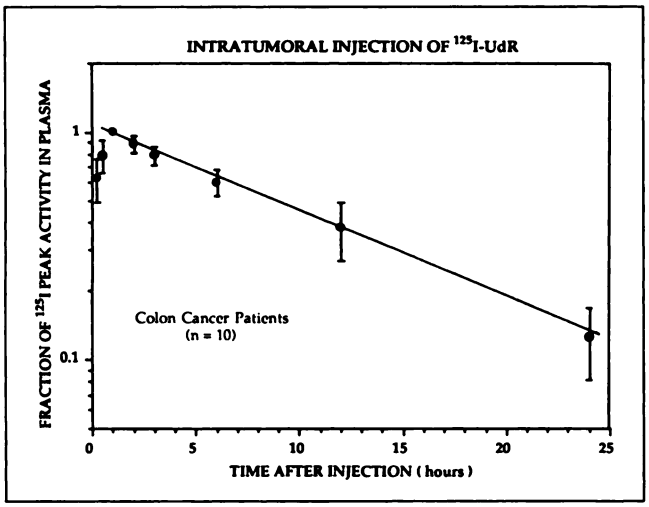

FIGURE 4. Semilogarithmic plot of mean values (±1 s.d.) for plasma radioactivity concentrations observed after intratumoral injection of [^{125}I]IUdR (normalized in each patient to corresponding peak activity). Equation of function interpolating all experimental points from peak time onward (see plot): $y = 1.0572e^{-0.0887t}$, $r = 0.998$; $p < 0.001$).

higher than that most commonly observed following systemic administration of radiolabeled antitumor monoclonal antibodies (range 0.001–0.01 %ID/g) (*41*). It should also be noted that such favorable tumor targeting in vivo is achieved by injecting a radioactive tracer that has virtually no mass (it is on the order of 10^{-14} g or 10^{-17} moles), as compared to the intravenous infusion of unlabeled IUdR or 5-bromo-2′-deoxyuridine in gram amounts (or 10^{-3} moles) in order to achieve incorporation by sufficient dividing tumor cells so as to be detected by immunohistochemistry. Furthermore, the very high levels of radioactivity incorporated in tumor compared with surrounding colonic tissue indicate that a more than satisfactory level of tumor targeting has been attained in these patients. In particular, radioactivity incorporation by normal dividing tissues located both adjacent to and outside the area directly involved by the intratumoral injection (such as transitional colonic epithelium and the bone marrow, respectively) is extremely low. On the other hand, metabolic clearance of [^{125}I]IUdR is extremely fast. At 24 hr postinjection, virtually no radioactivity is associated with parenchymal cells involved in the degradation process (i.e., the hepatocytes). The fast metabolic clearance of [^{125}I]IUdR drained from the injection site into circulating blood also prevents any significant uptake by dividing cells in the body, including tumor cells, relatively distant from the injection site.

The high tumor-to-nontumor ratios and the intranuclear incorporation of radioactivity were confirmed by microautoradiography. In addition, microautoradiographs demonstrate that radioactive incorporation is highest at the injection site, while simultaneously showing that tracer distribution within the entire tumor mass is, as expected, uneven; this makes intratumoral injection an unsuitable modality of locoregional administration if the goal is to achieve homogeneous distribution of the radiopharmaceutical within the tumor. On the other hand, even within areas with high levels of associated radioactivity, there are nests of tumor cells that show a lesser degree of incorporation, probably reflecting the well known heterogeneity of proliferative activity within any given tumor. The fraction of tumor cells that show incorporation of radioactivity at the injection site is very high (at least 15% to over 50% of these cells) and is consistently higher than the tumor labeling index values most commonly reported for colorectal cancer (rarely higher than 20%) following a 30-min in vitro incubation of surgical or biopsy tissue samples with triti-

ated TdR (*42–47*). It should be pointed out, however, that [^{125}I]IUdR incorporation by tumor cells did not correlate with tumor grading at histology as was previously reported for the tritiated TdR incorporation index (*48,49*). In addition, there does not seem to be a correlation between injected dose and level of uptake.

A comparison of the data in this study with those from a breast cancer study (*50*) indicates that the uptake values are lower in the latter case in which the tumor is characterized by low cell-proliferation kinetics. When plotting the percent of tumor cells showing radioactivity incorporation versus the fraction of injected dose taken up by the lesions, a highly significant positive correlation is found in both of these patient populations (Fig. 5).

Most of the [^{125}I]IUdR escaping immediate intracellular incorporation is likely to be transferred to the liver via the portal veins within minutes after injection, as indicated by the early appearance of radioactivity in the blood (peaking at 1 hr mostly in the form of metabolized tracer). Thus, diffusion of the tracer through the tumor is on the order of 15–45 min at most; this actually represents more of a "pulse" than an "infusion" type of exposure of tumor cells to [^{125}I]IUdR. These considerations also apply to a certain extent to the spatial component of the exposure of tumor cells to the injected tracer. In fact, notwithstanding all possible differences in vascularity, vascular permeability, blood flow and intratumoral metabolism among different patients, all cases consistently exhibited the same pattern of appearance and clearance of radioactivity in circulating fluids, with narrow coefficients of variation at all time points (Fig. 4). A minor fraction of the [^{125}I]IUdR injected intratumorally may be drained through a more slowly clearing system, a situation similar to that observed after intramuscular administration of radioiodinated IUdR (*51*). This remaining component might label cells entering the S phase and account for the high labeling indices observed in the patients' tumors and might explain the late appearance of some undegraded [^{125}I]IUdR at the 3-hr time point.

Since IUdR belongs to the class of drugs undergoing rapid first-pass hepatic degradation (*21,51–53*), most of the tracer flowing through the liver is rapidly deiodinated, and radioactivity is released into the circulation in the form of free [^{125}I]iodide which subsequently is excreted in the urine. Following the peak of plasma radioactivity attained 1 hr after intratumoral injection of [^{125}I]IUdR (Fig. 4), the curve is virtually superimposable on that observed following systemic bolus injection of free radioiodide (*54,55*), which has a plasma half-life of about 6 hr (versus about 8 hr for total plasma radioactivity in our patients) and a slope of about 0.1 hr^{-1} (versus about 0.09 hr^{-1} in our patients). These findings are consistent with the extravascular administration of a parent drug whose main metabolic pathway is removal from the body by deiodination and subsequent excretion through the kidneys. However, within the first 24 hr after injection, a certain fraction of the drug escapes deiodinative catabolism and is directly excreted in the urine.

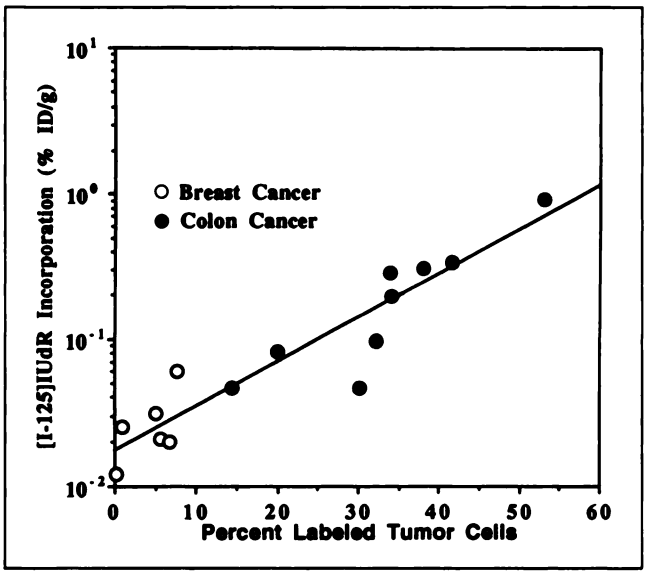

FIGURE 5. Semilogarithmic plot of percent of tumor cells showing radioactivity incorporation above background versus fraction of injected [^{125}I]IUdR dose per gram of tumor observed in the patients with colon cancer (closed circles) and in patients with breast cancer (open circles, from ref. *50*). Equation of function interpolating all experimental points combined (see plot): $y = 0.0172 \times 10^{+0.0303x}$; $r = 0.935$; $p < 0.001$). The radioactivity incorporation values (both as percent of labeled cells and as fraction of ID/g of tissue) correspond for each patient to the areas with the highest incorporation.

The urinary recovery of administered radioactivity obtained in this study is about 70% over 3 days, with minimal additional amounts up to the fifth day postinjection. Such a low value might be explained by the incomplete recovery of the tracer leaking in the intestinal lumen at the moment of injection (however meticulous the collection of colonic washing fluid may have been), resulting in spuriously high estimates of the dose actually injected. However, the ratio of peak activity in plasma (i.e., 1 hr postinjection) to injected dose observed in this study (4–6 %ID/liter) is within the same range as that observed in a parallel study involving percutaneous injection of [^{125}I]IUdR in patients with breast cancer (4.96 ± 1.08 %ID/liter), a strictly controlled condition that allows accurate estimate of the dose injected (*50*). Therefore, some excretion of radioactivity through the bile may also be assumed, as supported by the observations made in the two patients where this information was available. Thus, parenchymal liver cells may metabolize [^{125}I]IUdR not only by deiodination, but also through conjugation and biliary excretion of the radiopharmaceutical.

CONCLUSION AND PERSPECTIVES

The overall results obtained in this study fulfill the specific, limited goals of the experimental design. In particular, following a single intratumoral injection of [^{125}I]IUdR, we were able to demonstrate by differential tissue counting high concentrations of radioactivity in the tumor and high tumor-to-nontumor ratios, which reflect the high cell proliferation characteristic of these colorectal tumors. Mi-

croautoradiography showed that such tumor accumulation is linked specifically to intranuclear localization of radioactivity. Furthermore, analysis of the metabolic fate of [^{125}I]IUdR confirmed the rapid degradation of the radiopharmaceutical in vivo, thus minimizing its uptake by normal dividing tissues outside the injection area.

Our current studies represent a preliminary effort to demonstrate that locoregional administration of radioiodinated IUdR results in good tumor targeting in a tumor characterized by a high cell proliferation rate, at least within the limited tissue space directly involved with the injection ([^{125}I]IUdR incorporation within the tumor is in fact confined to a limited volume around the injection site). We do not intend, however, to suggest that colorectal cancer is a clinical situation where the tumor-targeting potential of radioiodinated IUdR can be usefully exploited by intratumoral injection.

Prospective applications in humans of locoregional administration of radioiodinated IUdR should be considered only where three essential requirements can be met: (a) achievability of homogeneous tracer distribution within the entire tumor; (b) availability of the tracer throughout several tumor-cell growth cycles in order to target virtually all tumor cells over a given period; (c) high cell proliferation kinetics in order to maximize the tumor-to-nontumor incorporation ratio. The first two of these requirements can be satisfied in part by certain locoregional administrations of radiolabeled IUdR, e.g., intracavitary instillation and intra-arterial infusion. The first modality is exemplified by the intraperitoneal administration of radioiodinated IUdR in patients with early peritoneal spread from ovarian carcinoma or endometrial cancer. This approach represents a logical transfer to humans of the experience acquired with the animal tumor model of ascites ovarian cancer (*3*). Metastatic lesion size represents an important limiting factor with this approach because homogeneous tracer distribution is only achievable in very small (0.5–1 mm) tumor lesions. The second modality involves patients with primary or metastatic liver disease in whom a catheter connected with a subcutaneous reservoir has been implanted in the hepatic artery as a route for locoregional chemotherapy. Again, the pattern of intratumor microcirculation might limit the possibility of achieving homogeneous tracer distribution within bulky tumor lesions. If these limitations on the possibility of attaining homogenous distribution of tracer within tumor lesions are taken into account, both intracavitary and intra-arterial administration would allow repeat injection or constant infusion regimens aimed at targeting most of the tumor cells, which are asynchronously progressing through the mitotic cycle.

In particular, patients with liver metastases from colorectal cancer appear to constitute a suitable model for testing the tumor-targeting potentials of radioiodinated IUdR, especially since this tumor usually displays high cell proliferation kinetics (*42–47*), thus also meeting the third requirement. We are therefore planning to initiate a pilot study to evaluate by external gamma camera imaging the dosimetry and optimal dosing regimen of tracer doses of ^{123}I-labeled IUdR (2–5 mCi range) infused into the hepatic artery of patients with liver metastases from colorectal cancer.

ACKNOWLEDGMENTS

This work was supported in part by Sorin Biomedica SpA, Saluggia, Italy; by grants from the Italian National Research Council (CNR, Rome), "Bilateral Projects" no. 91.00423.CT04; from the Italian Association for Research on Cancer, AIRC, Milan, no. 526/92; and by "Fondi per la Ricerca Scientifica 60%" from the Italian Ministry of Public Education, Rome, Italy. Sonia Di Sacco is the recipient of a research fellowship granted by the Italian Association for Research on Cancer, AIRC, Milan. The authors thank Mr. Mauro Dalcò for his precious help in performing the endoscopies and Drs. Francesco D'Elia, Pier Cristoforo Giulianotti, Aldo Guadagni and Luca Mannocci for patient care during their hospitalization at the Institute of General and Vascular Surgery of the University of Pisa.

Presented in part at the 38th Annual Meeting of the Society of Nuclear Medicine, Cincinnati, OH, June 11–14, 1991.

REFERENCES

1. Kassis AI, Van den Abbeele AD, Wen PYC, et al. Specific uptake of the Auger electron-emitting thymidine analogue 5-[^{123}I/^{125}I]iodo-2'-deoxyuridine in rat brain tumors: diagnostic and therapeutic implications in humans. *Cancer Res* 1990;50:5199–5203.
2. Mariani G, Guadagni A, Cei A, et al. Fate of 5-[I-125]iodo-2'-deoxyuridine injected intratumorally in patients with colon cancer [Abstract]. *J Nucl Med* 1991;32:1082–1083.
3. Baranowska-Kortylewicz J, Makrigiorgos GM, Van den Abbeele AD, Berman RM, Adelstein SJ, Kassis AI. 5[^{123}I]Iodo-2'-deoxyuridine in the radiotherapy of an early ascites tumor model. *Int J Radiat Oncol Biol Phys* 1991;21:1541–1551.
4. Mariani G, Cei A, Giuliani L, et al. Tumor targeting potential and metabolism of 5[^{125}I]iodo-2'-deoxyuridine injected intratumorally in patients with gastrointestinal or breast cancers [Abstract]. *J Nucl Biol Med* 1992;36:154–157.
5. Van den Abbeele AD, Baranowska-Kortylewicz J, Adelstein SJ, et al. Diagnostic and therapeutic applications of Auger-electron-emitting 5-[^{123}I/^{125}I]iodo-2'-deoxyuridine in cancer. In: Howell RW, Narra VR, Sastry KSR, Rao DV, eds. *Biophysical aspects of Auger processes*. AAPM Symposium Series No. 8. New York: AAPM; 1992:372–395.
6. Eidinoff ML, Cheong L, Rich MA. Incorporation of unnatural pyrimidine bases into deoxyribonucleic acid of mammalian cells. *Science* 1959;129:1550–1551.
7. Prusoff WH. Synthesis and biological activities of iodo-deoxyuridine, an analogue of thymidine. *Biochim Biophys Acta* 1959;32:295–296.
8. Commerford SL. Biological stability of IUdR labeled with ^{125}I after incorporation into the DNA of the mouse. *Nature (London)* 1965;206:949–950.
9. Sneider TW, Potter VR. Alternative de novo and 'salvage' pathways to thymidine triphosphate synthesis: possible implications for cancer chemotherapy. *Cancer Res* 1969;29:2398–2403.
10. Kassis AI, Sastry KSR, Adelstein SJ. Kinetics of uptake, retention, and radiotoxicity of ^{125}IUdR in mammalian cells: implications of localized energy deposition by Auger processes. *Radiat Res* 1987;109:78–89.
11. Erickson RL, Szybalski W. Molecular radiobiology of human cell lines. III. Radiosensitizing properties of 5-iododeoxyuridine. *Cancer Res* 1963;23:122–130.
12. Djordjevic B, Szybalski W. Genetics of human cell lines. III. Incorporation of 5-bromo and 5-iododeoxyuridine into the deoxyribonucleic acid of the human cell and its effect on radiation sensitivity. *J Exp Med* 1960;112:509–531.
13. Kinsella TJ, Dobson PP, Mitchell JB, Fornace AJ. Enhancement of x-ray induced damage by pretreatment with halogenated pyrimidine analogues. *Int J Radiat Oncol Biol Phys* 1987;13:733–739.
14. Jackson D, Kinsella TJ, Rowland J, et al. Halogenated pyrimidines as radiosensitizers in the treatment of glioblastoma multiforme. *Am J Clin Oncol* 1987;10:437–443.

15. Eidinoff ML, Cheong L, Gambetta Gurpide E, Benua RS, Ellison RR. Incorporation of 5-iodouracil labelled with iodine-131 into the deoxyribonucleic acid of human leukaemic leucocytes following in vivo administration of 5-iododeoxyuridine labelled with iodine-131. *Nature* 1959;183:1686–1687.
16. Prusoff WH, Jaffe JJ, Gunther H. Studies in the mouse of the pharmacology of 5-iododeoxyuridine, an analog of thymidine. *Biochem Pharmacol* 1960; 3:110–121.
17. Welch AD, Jaffe JJ, Cardoso SS, et al. Studies on the pharmacology of 5-iododeoxyuridine in animals and man. *Proc Am Assoc Cancer Res* 1960; 3:161.
18. Calabresi P, Cardoso SS, Finch SC, et al. Initial clinical studies with 5-iodo-2′-deoxyuridine. *Cancer Res* 1961;21:550–559.
19. Gitlin D, Commerford SL, Amsterdam E, Hughes WL. X-rays affect the incorporation of 5-iododeoxyuridine into deoxyribonucleic acid. *Science* 1961;133:1074–1075.
20. Prusoff WH. A review of some aspects of 5-^{125}I-iododeoxyuridine and azauridine. *Cancer Res* 1963;23:1246–1259.
21. Klecher RW Jr, Jenkins JF, Kinsella TJ, Fine RL, Strong JM, Collins JM. Clinical pharmacology of 5-iodo-2′-deoxyuridine and 5-iodouracil and endogenous pyrimidine modulation. *Clin Pharmacol Ther* 1985;38:45–51.
22. Kriss JP, Maruyama Y, Tung LA, Bond SB, Revesz L. The fate of 5-bromodeoxyuridine, 5-bromodeoxycytidine, and 5-iododeoxycytidine in man. *Cancer Res* 1963;23:260–268.
23. Philip PA, Bagshawe KD, Searle F, et al. In vivo uptake of ^{131}I-5-iodo-2-deoxyuridine by malignant tumours in man. *Br J Cancer* 1991;63:134–135.
24. Bloomer WD, Adelstein SJ. 5-^{125}I-Iododeoxyuridine as prototype for radionuclide therapy with Auger emitters. *Nature* 1977;215:620–621.
25. Dawson PA, Filipe MI. An ultrastructural and histochemical study of the mucous membrane adjacent to and remote from carcinoma of the colon. *Cancer* 1976;37:2388–2398.
26. Maskens AP, Deschner EE. Tritiated thymidine incorporation into epithelial cells of normal-appearing colorectal mucosa of cancer patients. *J Natl Cancer Inst* 1977;58:1221–1224.
27. Bleiberg H, Galand P. In vitro autoradiographic determination of cell kinetic parameters in adenocarcinomas and adjacent healthy mucosa of the human colon and rectum. *Cancer Res* 1976;36:325–328.
28. Bradley EW, Chan PC, Adelstein SJ. The radiotoxicity of iodine-125 in mammalian cells. I. Effects on the survival curve of radioiodine incorporated into DNA. *Radiat Res* 1975;64:555–563.
29. Wasternak C. Degradation of pyrimidines and pyrimidine analogs—pathways and mutual influences. *Pharmacol Ther* 1980;8:629–651.
30. Desgranges C, Razaka G, Rabaud M, Baricaud H, Balzarini J, de Clercq E. Phosphorolysis of (E)-5-(2-bromovinyl-2′-deoxyuridine (BVDU) and other 5-substituted-2′-deoxyuridines by purified human thymidine phosphorylase and intact blood platelets. *Biochem Pharmacol* 1983;32:3583–3590.
31. Charlton DE, Booz J. A Monte Carlo treatment of the decay of ^{125}I. *Radiat Res* 1981;87:10–23.
32. Kassis AI, Sastry KSR, Adelstein SJ. Intracellular localization of Auger electron emitters: biophysical dosimetry. *Radiat Prot Dosim* 1985;13:233–236.
33. Kassis AI, Fayad F, Kinsey BM, Sastry KSR, Taube RA, Adelstein SJ. Radiotoxicity of ^{125}I$^-$ in mammalian cells. *Radiat Res* 1987;111:305–318.
34. Painter RB, Young BR, Burki HJ. Non-repairable strand breaks induced by ^{125}I-incorporated into mammalian cells. *Proc Natl Acad Sci USA* 1974;71: 4836–4838.
35. Hofer KG, Harris CR, Smith JM. Radiotoxicity of intracellular ^{67}Ga, ^{125}I and ^{3}H. Nuclear versus cytoplasmic radiation effects in murine L1210 leukemia. *Int J Radiat Biol* 1975;28:225–241.
36. Hofer KG, Hughes WL. Radiotoxicity of intracellular tritium, iodine-125 and iodine-131. *Radiat Res* 1971;47:94–104.
37. Chan PC, Lisco E, Lisco H, Adelstein SJ. The radiotoxicity of iodine-125 in mammalian cells. II. A comparative study on cell survival and cytogenic responses to ^{125}IUdR, ^{131}IUdR and ^{3}HTdR. *Radiat Res* 1976;67:332–343.
38. Morris NR, Cramer JW. DNA synthesis by mammalian cells inhibited in culture by 5-iodo-2′-deoxyuridine. *Mol Pharmacol* 1966;2:1–9.
39. Bresnick E, Thompson UB. Properties of deoxythymidine kinase partially purified from animal tumors. *J Biol Chem* 1965;206:949–950.
40. Quackenbush RC, Shields AF. Local re-utilization of thymidine in normal mouse tissues as measured with iododeoxyuridine. *Cell Tissue Kinet* 1988; 21:381–387.
41. Fischman AJ, Khaw BA, Strauss HW. Quo vadis radioimmune imaging. *J Nucl Med* 1989;30:1911–1915.
42. McDonald GO, McIver JM, Llamas AJ, Sky-Peck HH. Tumor cytotoxicity. *Arch Surg* 1966;92:541–547.
43. McKinna JA. Access of drugs to tumours of the large intestine. *Proc Royal Soc Med* 1970;63:23–24.
44. Lesher S, Schiffer LM, Phanse M. Human colonic tumor cell kinetics. *Cancer* 1977;40:2706–2709.
45. Meyer JS, Prioleau PG. S-phase fractions of colorectal carcinomas related to pathologic and clinical features. *Cancer* 1981;48:1221–1228.
46. Ota DM, Drewinko B. Growth kinetics of human colorectal carcinoma. *Cancer Res* 1985;45:2128–2131.
47. Ponz de Leon M, Costa A, Lanza G Jr, et al. Reliability of ^{3}H-thymidine index: cell proliferation of colorectal carcinoma in three different centers. *Mod Pathol* 1991;4:627–631.
48. Bleiberg H, Buyse M, Van den Henle B, Galand P. Cell cycle parameters and prognosis of colorectal cancer. *Eur J Cancer Clin Oncol* 1984;20:391–396.
49. Rew DA, Wilson GD, Taylor I, Weaver PC. Proliferation characteristics of human colorectal carcinomas measured in vivo. *Br J Surg* 1991;78:60–66.
50. Mariani G, Giuliani L, Baranowska-Kortylewicz J, et al. Intratumoral injection of 5-[^{125}I]iodo-2′-deoxyuridine in patients with breast cancer. In: Hofer R, Bergmann H, Sinzinger H, eds. *Radioactive isotopes in clinical medicine and research*, 20th edition. Stuttgart-New York: Schattauer Verlag; 1992:188–193.
51. Clifton KH, Szybalski W, Heidelberger C, Gollin FF, Ansfield FJ, Vermund H. Incorporation of ^{125}I-labeled iododeoxyuridine into the deoxyribonucleic acid of murine and human tissues following therapeutic doses. *Cancer Res* 1963;23:1715–1722.
52. Hughes WL, Commerford SL, Gitlin D, et al. Deoxyribonucleic acid metabolism in vivo. I. Cell proliferation and death as measured by incorporation and elimination of iododeoxyuridine. *Fed Proc* 1964;23:640–648.
53. Belanger K, Klecher RW Jr, Rowland J, Kinsella TJ, Collins JM. Incorporation of iododeoxyuridine into DNA of granulocytes in patients. *Cancer Res* 1986;46:6509–6512.
54. De Groot LJ. Kinetic analysis of iodine metabolism. *J Clin Endocrinol* 1966;26:149–173.
55. Rosenthal D. Kinetic analysis of iodide and thyroxine metabolism in "hot" thyroid nodules. *Metabolism* 1981;30:384–392.